

# Overview of Multilayered Thin Film Theories for MEMS and Electronic Packaging Applications

Chih-Tang Peng<sup>1</sup>, Kuo-Ning Chiang<sup>2</sup>

E-Mail: [Knchiang@pme.nthu.edu.tw](mailto:Knchiang@pme.nthu.edu.tw)

Department of Power Mechanical Engineering  
National Tsing Hua University  
Hsin Chu, Taiwan 300, R.O.C.

## Abstract

Interfacial stresses due to thermal mismatch in layered structures are one of the major causes of mechanical failures in electronic packages and Micro-Electro-Mechanical System (MEMS) structures. Applying analytical solutions to predict the magnitude and the distribution of interfacial stresses in thermostat-like multilayer structures has been widely adopted by many electronic packaging and MEMS researchers.

This investigation is based on multilayer theory models. To discuss and distinguish their characteristics, finite element analysis numerical solutions and multilayer theory analytical solutions are compared and analyzed. This encompasses the theories' application spectrum as well as their prediction ability. This work not only discusses the property and the workability of theories but also fabricates a multilayer structure made by silicon substrate to demonstrate the feasibility of finite element method (FEM) and multilayer theories experimentally. Experimental result demonstrates that finite element method is a feasible approach to predict the mechanical behavior of multilayer structures.

Keywords: Finite element analysis, Multilayer theory, Electronic package, MEMS

## . Introduction

Calculating interfacial stresses via multilayer theories to predict the reliability of electronic packaging and MEMS structures has been widely employed for years. Figure 1 indicates a flip-chip package.

An equivalent method could be applied to this package to form a trilayer thermostat structure. Hence multilayer theories can predict its reliability and mechanics behavior. Figure 2 illustrates a MEMS piezoresistive sensor. A laminated plate structure with piezoresistive elements on this sensor can sense the stress change due to pressure loading. The laminated plate can be simplified to a multilayer structure. Therefore multilayer theories can also apply to the laminated plate MEMS structure to predict mechanics behavior during pressure loading. Currently, electronic

package and MEMS structures have become much smaller and thinner, thus the mesh density of finite element analysis is rising, and the CPU time required for computer simulation is consequently increasing. Multilayer theory has the distinguishing characteristic of fast calculation. Thus their analytical solutions require less time than finite element analysis numerical solutions do.

Timoshenko [1] first examined the mechanical behavior of bimetal thermostat based on an elementary beam theory. In Timoshenko's theory, the concept of continuous displacement between the interfaces evolved into a basic hypothesis of numerous other theories. Basis on Timoshenko's model, Matthys [2] proposed "Timoshenko joined beams bimetal thermostat model" for the shearing stress and normal force prediction at the interface of a bilayer structure. Suhir developed two models - Suhir [3] and Suhir extended [4] to predict the shearing stress as well as peeling stress at the interface between two different materials, both these two models are based on Timoshenko's bimetal thermostat theory. A very long (or thin) and linear behavior structure is required in Suhir [3] model. Notably, it is the first model to calculate the interfacial peeling stress of a thermostat structure. Suhir modified some flaws of the previous model in a subsequent article: his second model-Suhir extended [4] enhanced the accuracy of interfacial stresses prediction. Jiang [5] proposed a distinct model to predict the interfacial stresses, which includes two different material beam structures that have a very thin adhesive layer between the interfaces. Jiang's model is based on the conventional trilayer thermostat theories that are proposed by Chen [6], Chen [7] and Delale [8]. According to Jiang's theory, Wang [9] presented a model to predict the interfacial and die cracking stress. The governing equations of Wang's and Jiang's models are similar, however the distinguishing feature of the former is that the length of bottom layer can be changed; thereby Wang's model is more analogous to real electronic packaging structures. Basis on Suhir's theory, Pao [10] produced a multilayer structure model to predict peeling and shearing stress between each interface. In Pao's article, Pao derived the governing equations and applied the analytical results to predict the

---

<sup>1</sup> . Graduate Assistant, Ph.D candidate

<sup>2</sup> . Corresponding Author, Associate Professor, Dept. of Power Mechanical Engineering, National Tsing Hua University

interfacial stresses of trilayer and five-layer structure.

### . Multilayer analytical models

#### (1) Timoshenko joined beams bimetal thermostat model

Matthys [2] proposed Timoshenko's joined beams bimetal thermostat model, which is an extension of Timoshenko's Bimetal thermostat theory. Figure 3 illustrates the dimension parameters of Timoshenko's joined beams model. The equation of interfacial stress is presented as follows:

$$q(x) = C \mathbf{d}(x+L) - C \mathbf{d}(x-L) \quad (1)$$

$$C = \frac{(\alpha_1 - \alpha_2)}{\left(\frac{1 - \nu_1^2}{E_1 b h_1} + \frac{1 - \nu_2^2}{E_2 b h_2} + \frac{h^2}{4bD}\right)}$$

where  $q(x)$  is interfacial shearing stress,  $L$  is half length of the structure,  $b$  is width of the structure,  $h_1$  and  $h_2$  are the thickness of top layer and bottom layer,  $h=(h_1+h_2)$ ,  $E_1$  and  $E_2$  are Young's modulus of top layer and bottom layer,  $\nu_1$  and  $\nu_2$  are poisson's ratio, and  $D=D_1+D_2=E_1 h_1^3/12(1-\nu_1^2)+E_2 h_2^3/12(1-\nu_2^2)$ .

Timoshenko's joined beams bimetal thermostat model predicts only interfacial shearing stress. That is, it does not analyze interfacial peeling stress. Thus, a few analyses of physical phenomena are not sufficient in this model.

#### (2) Suhir's model [3]

Based on Timoshenko's theory, Suhir presented the bimetal thermostat model, which improves several assumptions of Timoshenko's model. Therefore Suhir's model can predict both shearing and peeling stresses. Figure 3 illustrates the dimension parameters of Suhir's model. Interfacial stress equations are presented as follows:

$$q(x) = -\frac{kb\Delta\alpha\Delta T}{I \cosh(kL)} \sinh(kx) \quad (2)$$

$$p(x) = -\frac{D_1 h_2 - D_2 h_1}{2D} \frac{b\Delta\alpha\Delta T}{k \cosh(kL)} \cosh(kx) \quad (3)$$

where  $q(x)$  is shearing stress and  $p(x)$  is peeling stress,  $L$  is half length of the structure,  $b$  is width of the structure,  $h_1$  and  $h_2$  are the thickness of top layer and bottom layer,  $h=(h_1+h_2)$ ,  $\alpha_1$  and  $\alpha_2$  are coefficient of temperature

expansion (CTE),  $\Delta T$  is temperature change,  $D=D_1+D_2=E_1 h_1^3/12(1-\nu_1^2)+E_2 h_2^3/12(1-\nu_2^2)$ ,  $E_1$  and  $E_2$  are Young's modulus of top layer and bottom layer,  $\nu_1$  and  $\nu_2$

$$\text{are poisson's ratio, and } k^2 = \frac{\lambda}{\kappa},$$

$$\kappa = b(\kappa_1 + \kappa_2) = \frac{2(1+\nu_1)h_1}{3E_1} + \frac{2(1+\nu_2)h_2}{3E_2},$$

$$\lambda = \frac{1 - \nu_1^2}{E_1 b h_1} + \frac{1 - \nu_2^2}{E_2 b h_2} + \frac{h^2}{4bD}.$$

Although Suhir's model contains a few flaws, the analytical methodology established by Suhir is adopted by many researchers. No matter in theory development or experiment analysis, Suhir contributes much to multilayer thermostat theories.

#### (3) Suhir extend model [4]

Based on his previous model, in 1989 Suhir proposed

another model. This model enhances some assumptions regarding the peeling effect. The dimension parameters of Suhir extended model are illustrated in Fig. 3, and the equations of interfacial stresses are presented as follows:

$$q(x) = C_1 \sinh \mathbf{b}_1 x + C_3 \cosh \mathbf{g}_1 x \sin \mathbf{g}_2 x + C_5 \sinh \mathbf{g}_1 x \cos \mathbf{g}_2 x \quad (4)$$

$$p(x) = C_2 \cosh \mathbf{b}_1 x + C_4 \cosh \mathbf{g}_1 x \cos \mathbf{g}_2 x + C_6 \sinh \mathbf{g}_1 x \sin \mathbf{g}_2 x \quad (5)$$

where  $q(x)$  is shearing stress and  $p(x)$  is peeling stress, and  $C_1 \sim C_6$ ,  $\mathbf{b}_1$ ,  $\mathbf{g}_1$ ,  $\mathbf{g}_2$  are constants (detail parameters are defined in Suhir extend [4]) that are composed of material properties, dimension parameters and temperature change, respectively.

Eqs. (4) and (5) are composed by hyperbolic sine and cosine, respectively. Notably, the interfacial stress equations in Suhir's extended model are more complicated than those in his first model are. Owing to its complex calculating process, Suhir's extended model requires more time than other theories do in practical applications.

#### (4) Jiang's model

This is a trilayer thermostat model, which has two beam structures comprised of separate material and a very thin adhesive layer between the interfaces. The dimension parameters of Jiang's model are illustrated in Fig. 4, Interfacial stress equations are as follows:

$$q(x) = \frac{G_a}{h_a \lambda} [(1 + \nu_1)\alpha_1 - (1 + \nu_2)\alpha_2] \Delta T \times \exp[\lambda(x - L)] \quad (6)$$

$$\lambda = 2 \sqrt{\frac{G_a}{h_a} \left( \frac{1}{E_1' h_1} + \frac{1}{E_2' h_2} \right) \frac{L - x}{\sqrt{h_a(h_1 + h_2)}}}$$

$$p(x) = \mathbf{s}_0 \left\{ e^{I(x-L)} - e^{c(x-L)} \left[ \frac{I^2}{2c^2} \sin[c(x-L)] + \left( \frac{I^2}{2c^2} + \frac{2c}{I} \right) \cos[c(x-L)] \right] \right\} \quad (7)$$

$$\sigma_0 = \frac{3 \left( \frac{1}{E_1' h_1^2} - \frac{1}{E_2' h_2^2} \right) [(1 + \nu_1)\alpha_1 - (1 + \nu_2)\alpha_2] \Delta T}{4(1 - \nu_a) \left( \frac{1}{E_1' h_1} + \frac{1}{E_2' h_2} \right)^2 + 6 \left( \frac{1}{E_1' h_1^3} + \frac{1}{E_2' h_2^3} \right) \frac{h_a}{G_a}}$$

$$\chi = \left[ 3 \frac{E_a'}{h_a} \left( \frac{1}{E_1' h_1^3} + \frac{1}{E_2' h_2^3} \right) \right]^{1/4}$$

where  $q(x)$  is shearing stress and  $p(x)$  is peeling stress,  $L$  is half length of the structure,  $h_1$ ,  $h_a$  and  $h_2$  are the thickness of top layer, adhesive layer and bottom layer,  $E_1$ ,  $E_a$  and  $E_2$  are Young's modulus,  $\nu_1$ ,  $\nu_a$  and  $\nu_2$  are CTE,  $\alpha_1$ ,  $\alpha_a$  and  $\alpha_2$  are poisson's ratio,  $G_a = E_a/2(1+\nu_a)$  is shear modulus of adhesive layer,  $E_i' = E_i/(1-\nu_i^2)$ , ( $i=1,2$ ),  $E_a' = E_a/(1-\nu_a^2)$ ,  $\Delta T$  is temperature change.

Jiang's trilayer model differs from Suhir's in that it is based on conventional trilayer thermostat theories, which can be applied more extensively.

### (5) Wang's model

According to Jiang's theory, Wang presented a model to predict the interfacial and die cracking stresses. The distinguishing feature of this theory is that the length of the bottom layer can be altered hence it is more analogous to real electronic packaging structures. Figure 5 depicts the dimension parameters of Wang's model. Its interfacial stress equations are as follows:

$$q(x) = A \exp [I(x - L_1)] , \quad L_1 > x > 0 \quad (8)$$

$$\lambda = 2 \sqrt{\frac{G_a}{h_a} \left( \frac{1}{E_1' h_1} + \frac{1}{E_2' h_2} \right)}$$

$$p(x) = \beta A \exp [\lambda(x - L_1)] + \exp [\chi(x - L_1)] \{ B \sin [\chi(x - L_1)] + C \cos [\chi(x - L_1)] \}$$

$$, \quad L_1 > x > 0 \quad (9)$$

$$\beta = \frac{3 \left( \frac{1}{E_1' h_1^2} - \frac{1}{E_2' h_2^2} \right) \frac{h_a}{G_a} \lambda}{4(1 - \nu_a) \left( \frac{1}{E_1' h_1} + \frac{1}{E_2' h_2} \right)^2 + 6 \left( \frac{1}{E_1' h_1^3} + \frac{1}{E_2' h_2^3} \right) \frac{h_a}{G_a}}$$

$$\chi = \left[ 3 \frac{E_a'}{h_a} \left( \frac{1}{E_1' h_1^3} + \frac{1}{E_2' h_2^3} \right) \right]^{1/4}$$

Parameters A, B, and C are determined by two types of boundary conditions:

#### 1. Traction-free boundary condition:

It represents a single, isolated chip on a finite substrate.

$$A = \frac{G_a}{h_a \lambda} [(1 + \nu_1) \alpha_1 - (1 + \nu_2) \alpha_2] \Delta T , \quad B = - \frac{\lambda^2}{2 \chi^2} \beta A ,$$

$$C = - \left( \frac{\lambda^2}{2 \chi^2} + \frac{2 \chi}{\lambda} \right) \beta A$$

#### 2. Periodic boundary condition:

It represents uniformly distributed chips on a substrate.

$$A = \frac{\left[ \frac{L_2}{L_1} - \frac{E_1 h_1^3}{E_1' h_1^3 + E_2' h_2^3} \right] \frac{G_a}{h_a \lambda} [(1 + \nu_1) \alpha_1 - (1 + \nu_2) \alpha_2] \Delta T}{\frac{L_2}{L_1} - \frac{6 G_a}{E_s' h_s^2 h_a \chi^4} \left[ \beta \left( \frac{\lambda}{4} + \frac{\chi^4}{\lambda^3} \right) + \frac{1}{(1 - \nu_a) h_2} + \frac{\chi^4 h_2}{2 \lambda^2} \right]}$$

$$B = \frac{E_a'}{h_2 h_a c^2} [(1 + n_1) a_1 - (1 + n_2) a_2] \Delta T -$$

$$\left[ I^2 b + \frac{4 I}{(1 - n_a) h_2} \right] \frac{A}{2 c^2} , \quad C = B - \frac{2 c b}{I} A$$

where  $q(x)$  is shearing stress and  $p(x)$  is peeling stress,  $L_1$  is half length of the top layer, and other parameters are defined identically to Jiang's theory.

### (6) Pao's [10] model

Basis on Suhir's theory, Pao produced a multilayer structure model to predict interfacial stresses between each interface. Figure 6 presents Pao's model. Pao transformed interfacial stress calculations into an eigenvalue problem and applied a matrix to express interfacial stresses, thereby facilitating prediction of interfacial stresses within multilayer structures. Owing to the complex equations and matrices, the functions are not depicted here.

Pao's multilayer thermostat model provides an analytical solution for electronic packaging and MEMS applications. The character of multilayer calculations can accommodate more flexibility of structure reliability design.

## . Experimental validation

In order to demonstrate the feasibility of the finite element analysis (FEA) and multilayer theories, an experiment for multilayer thermostat displacement measurement is designed. A silicon base multilayer structure is fabricated and a measurement system is applied during the thermal loading process in the experiment. Owing to there is no proper instrument to measure interfacial stresses at the interfaces of a multilayer structure, a Twyman-Green interferometer is employed to measure the out of plane displacement of the fabricated structure. This experiment can assist researches to realize the mechanics behavior and some physical phenomena with multilayer structure. Figure 7 indicates the experiment procedure.

### (1) Thin multilayer structure fabrication

In this investigation, semiconductor process is applied to fabricate a nickel/silicon bilayer structure. Figure 8 presents the process flowchart. Two seed layers, gold and chromium, are sputtering on a silicon wafer for the electroplating process; subsequently a nickel layer is deposited on the seed layer via electroplating. Finally, a wafer slicing process is employed to construct a slender rectangular chip and thereby the bilayer structure is complete.

### (2) Twyman-Green interferometer measurement

The dimensions of the fabricated nickel/silicon bilayer structure are: length: 7.6mm, width: 1.6mm, nickel layer thickness: 178  $\mu$ m, and silicon layer thickness: 500  $\mu$ m. Figure 9 presents the cross section view of the structure. A Twyman-Green interferometer is applied to measure the out of plane displacement of this fabricated structure during thermal loading process. A vacuum oven is assembled on the Twyman-Green interferometer optical table to constitute a real time measurement system. The thermal loading conditions are from 25 to 40 , 25 to 50 , 25 to 60 , 25 to 70 , and room temperature is 25 .

Following measurement, the fringes of each thermal condition are depicted in Fig. 10 and each fringe express 0.316  $\mu$ m out of plane displacement. In this work, the out of plane displacement offset from structure edge to the center is selected in order to compare with FEA. The square point line in Fig. 11 illustrates the displacement offset value after converting fringes into numeral.

### (3) Experiment and finite element analysis comparison

To demonstrate the feasibility and the accuracy of FEA, the experimental data is compared to the finite element numerical solution. In this work, the ANSYS finite element program is employed. A two-dimensional four-node element is adopted for the analysis. Table 1 lists the material properties of nickel and silicon. The finite element model (Fig. 12) has 420 elements, and a boundary condition is with one node fixed in both the x and y direction at the center of the top surface.

Figure 11 illustrates a comparison of out of plane displacement offset between FEA and the experiment. It is observed that the FEA gave a promise result with the

experimental value, thereby demonstrating that FEA can predict the mechanics behavior of multilayer structures. Based on the above demonstration, FEA numerical method is applied in the next section to verify the multilayer theories.

### . Multilayer theories and numerical solutions comparison

The finite element method is employed to verify the expressions of interfacial shearing and peeling stresses in multilayer theories. In this comparison, the theories are divided into two classifications, based on their characteristics: bilayer linear structure (Suhir, Suhir extend, Jiang, Wang and Timoshenko “joined beam” theories) and trilayer linear structure (Jiang, Wang and Pao theories). The ANSYS finite element program is employed. As well, a two-dimensional four-node element is adopted in this analysis.

#### ● Bilayer linear structure

The following example is executed for a comparison:

The numerical example is performed on a copper/silicon bilayer structure. The length of this bilayer structure is 2 cm, the thickness of upper copper layer is 0.025 cm and the thickness of bottom silicon layer is 0.05 cm. Thermal loading is 100 and stress free temperature is 25 . Table 2 lists the material properties of copper and silicon. To catch the stress concentration effect at the free edge, the finite element model has 600 elements. Its boundary condition has one node that is fixed in both the x and y direction at the center of bottom surface.

The calculated shearing and peeling stresses are plotted in Fig.13 and Fig.14. Based on this investigation, some conclusions is expressed as follows:

#### (1) Interfacial shearing stress:

Suhir, Suhir extend, Jiang, Wang and Timoshenko “joined beam” theories can be applied on a bilayer linear structure for shearing stress predictions. It is found that Timoshenko’s “joined beam” theory is not suitable to predict the distribution of interfacial shearing stress as it simply calculates the interfacial shearing stress at the edge. Suhir, Suhir extend, Jiang and Wang’s theories are more conformable to FEA in this example. Due to an effect referred to as “edge effect”, the shearing stresses at the edge in Suhir’s, Jiang’s and Wang’s theories have much discrepancy in magnitude and have an opposite sign when they are compared to the FEA data. Although there are some mismatches in magnitude between Suhir’s extended theory and FEA, their trend of shearing stress distribution is similar. Therefore, Suhir’s extended theory is a better model to predict interfacial stress in this investigation.

#### (2) Interfacial peeling stress:

Due to the theory’s limitations, Timoshenko’s “joined beam” theory cannot predict peeling stress, thus it is excluded from Fig. 14. The peeling stress distribution trend in Suhir’s extended theory conflicts with that of FEA. However, the Suhir, Jiang and Wang theories correlate well with FEA.

According to the above conclusions, the shearing and

peeling stresses calculated from the various theories varying significantly. Various combinations of dimension and materials produce the differing findings. Proper selection of multilayer theories can enhance the accuracy of prediction. Based on this viewpoint, a recommendation is presented in Table 3 for the edge effect solution in this example.

#### ● Trilayer linear structure

The following example is executed for a comparison: A numerical example is performed on a silicon/adhesive/FR-4 trilayer structure. The length of this bilayer structure is 2 cm, the thickness of upper silicon layer is 0.05 cm, the thickness of middle adhesive layer is 0.0025 cm, and the thickness of bottom FR-4 layer is 0.07 cm. Thermal loading is 100 , and stress free temperature is at 25 . Table 4 displays the material properties of silicon, adhesive and FR-4. The finite element model has 1000 elements, and its boundary condition has one node, which is fixed in both the x and y direction at the center of the bottom surface.

Figures 15 and 16 demonstrate the calculated shearing and peeling stresses. The following conclusions were attained from this investigation:

#### (1) Interfacial shearing stress:

Figure 15 reveals that due to the “edge effect”, the trend of shearing stress distribution in Jiang and Wang’s theory conflict with that of FEA. Although there is some difference in magnitude between Pao’s theory and FEA, their shearing stress distribution is similar. Thus, in this example, Pao’s theory is a better model to predict the interfacial stress.

#### (2) Interfacial peeling stress:

Figure 16 depicts that the trend of peeling stress distribution in Pao’s theory coincides with that of FEA, however a sign error occurs in this comparison at the free edge. In this example, Jiang and Wang’s theories are not only similar to the trend of FEA but also have the same characteristics at the free edge.

Basis on the above comparison, a recommendation is presented in Table 5 for Pao, Jiang and Wang’s theories prediction ability within a trilayer linear structure.

### . Conclusions

In this study, a multilayer structure is discussed based on theories, as well as numerical examples and experimentation. The following conclusions were derived:

1. Numerical and analytical comparisons were performed to discuss and distinguish the characters of multilayer theories for their application spectrum as well as prediction ability. Some recommendations were presented for theories’ prediction ability following comparison.
2. In a bilayer structure within thermal loading experiment, following measurement and analysis, it is found that the trend of out of plane displacement corresponds to that of FEA. Thus confirming that FEA can predict the mechanics behavior of multilayer structures, and that it is a reliable basic tool for multilayer theory demonstration.

In accordance with the above conclusions, proper selection of multilayer theories can increase the accuracy of

interfacial stress prediction within practical applications, and FEA is a distinguished method to predict the mechanical behavior of multilayer structures.

**Acknowledgements:**

The authors would like to thank the National Science Council of the Republic of China for financially supporting this research under Contract No. NSC89-2212-E-007-105.

**References**

[1] S.P.Timoshenko, Analysis of Bi-metal Thermostats, in: Journal of the Optical Society of America, Vol.11 (1925) 233-255.  
 [2] L.Matthys, An Analysis of an Engineering Model for the Thermal Mismatch Stresses at the interface of a Uniformly Heated Two Layer Structure, in: Journal of Microcircuits and Electronic Packaging, Vol.19 (1999) 323-329.  
 [3] E.Suhir, Stress in Bi-Metal Thermostats, in: ASME Journal of Applied Mechanics, Vol.53 (1986) 657-660.  
 [4] E.Suhir, Interfacial Stresses in Bimetal Thermostats, in: ASME Journal of Applied Mechanics, Vol.56 (1989)

595-600.  
 [5] Z.Q.Jiang, Y.Huang, and A.Chandra, Thermal Stresses in Layered Electronic Assemblies, in: ASME Journal of Electronic Packaging, Vol.119 (1997) 127-132.  
 [6] W.T.Chen, C.W.Nelson, Thermal Stress in Bonded Joints, in: IBM.J.Res.Develop., Vol.23 (1979) 178-188.  
 [7] D.Chen, S.Cheng, and T.D.Gerhart, Thermal Stresses in Laminated Beams, in: Journal of Thermal Stresses, Vol.23 (1982) 67-84.  
 [8] F.Delale, F.Erodgan, and M.N.Aydinoglu, Stresses in Adhesively Bonder Joints: A Close-Form Solution, in: Journal of Composite Materials, Vol.15 (1981) 249-271.  
 [9] K.Wang, Y.Huang, A.Chandra, and K.X.Hu, Interfacial Shear Stresses, Peeling Stress, and Die Cracking Stress in Trilayer Electronic Assemblies, in: IEEE Transactions on Components and Packaging Technologies, Vol.23, no.2 (June, 2000) 309-319.  
 [10] Y.H.Pao and Eisele, Interfacial Shear and Peel Stresses in Multilayered Thin Stacks Subjected to Uniform Thermal Loading, in: ASME Journal of Electronic Packaging, Vol.113, (1991) 164-172



Fig. 1: Multilayer theory on flip-chip package application

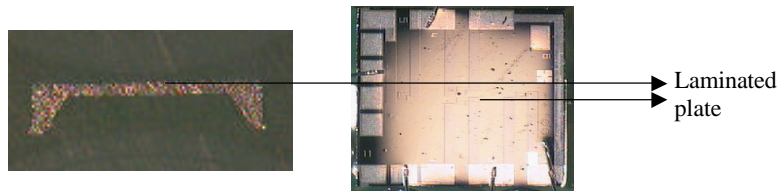


Fig. 2: Cross section view and top view of a MEMS piezoresistive sensor

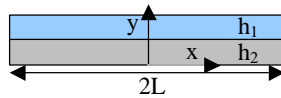


Fig. 3: Dimension parameters of Timoshenko, Suhir, and Suhir extend model

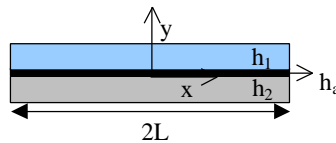


Fig. 4: Dimension parameters of Jiang's trilayer model

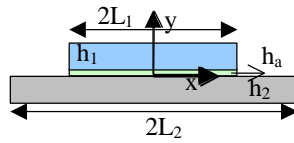


Fig. 5: Dimension parameters of Wang's trilayer model

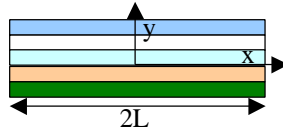


Fig. 6: Pao's multilayer model

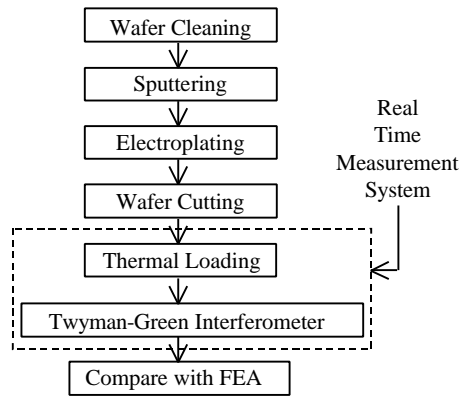


Fig. 7: Multilayer structures with thermal loading experiment procedure

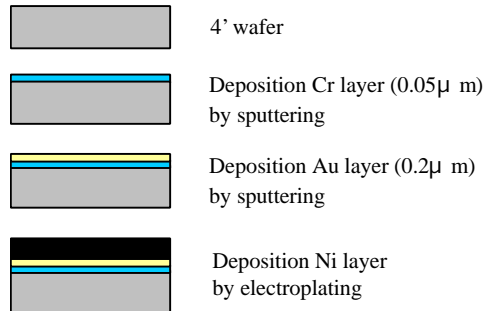


Fig. 8: Nickel/silicon bilayer structure fabrication process flowchart



Fig. 9: Cross section view of the nickel/silicon bilayer structure



Ni+Si bilayer structure at room temperature: 25

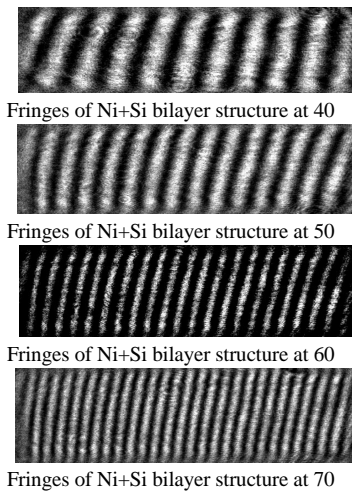


Fig. 10: The Twyman-Green interferometer fringes of each thermal loading

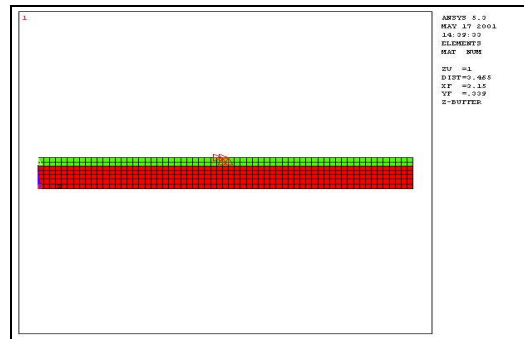
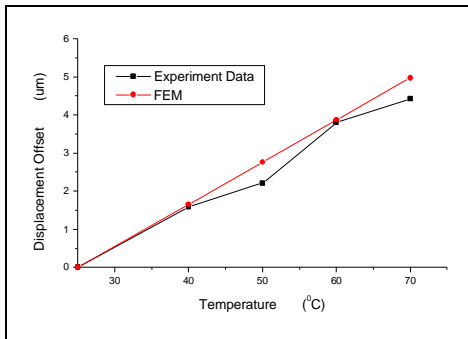


Fig. 11: Comparison result of out of plane displacement offset between FEA and experiment

Fig. 12: Finite element model of nickel/silicon bilayer structure

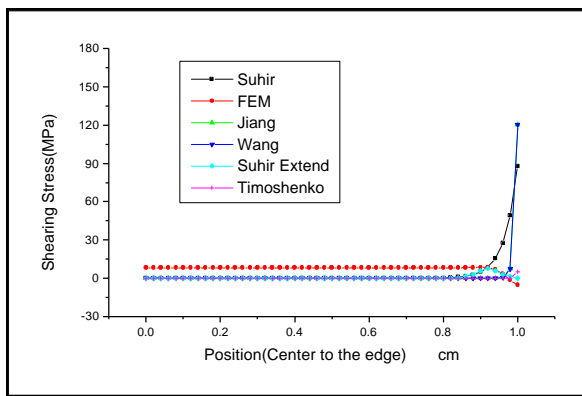


Fig. 13: The comparison of shearing stress between FEM and theories

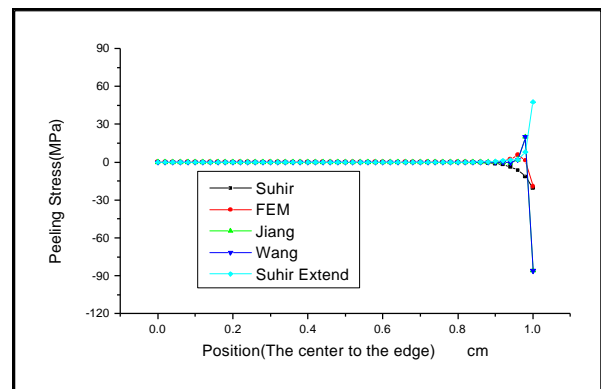


Fig. 14: The comparison of peeling stress between FEM and theories

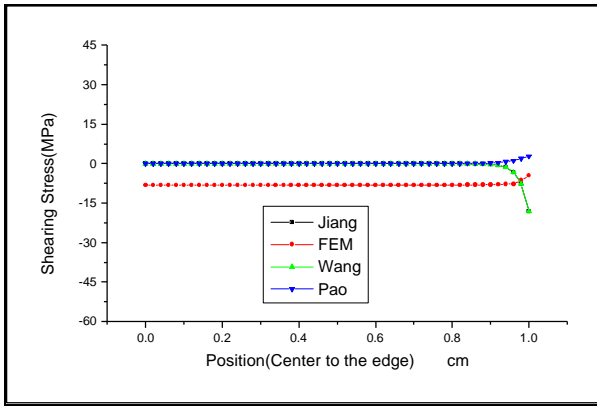


Fig. 15: The comparison of shearing stress between FEM and theories

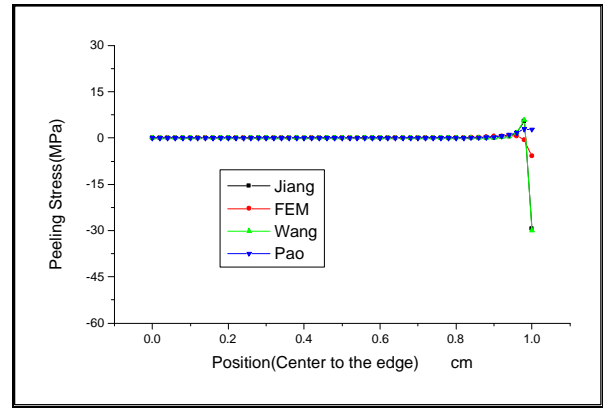


Fig. 16: The comparison of peeling stress between FEM and theories

Table 1. Material properties of nickel and silicon

Layer	Young's Modulus	Poisson's Ratio	CTE (1/ )
Nickel	207(Gpa)	0.31	11.1ppm
Silicon	112.4(Gpa)	0.28	2.62ppm

Table 2. Material properties of copper and silicon

Layer	Young's Modulus	Poisson's Ratio	CTE (1/ )
Copper	117(Gpa)	0.31	17ppm
Silicon	112.4(Gpa)	0.28	2.62ppm

Table 3. Theory prediction ability at the free edge in bilayer structure

Material Combination: Upper Layer (Copper)+Lower Layer (Silicon)					
Theory	Suhir	Suhir Extend	Jiang	Wang	Timoshenko
Shearing Stress	Not suitable	Better	Not suitable	Not suitable	Not suitable
Peeling Stress	Better	Not suitable	Better	Better	N/A

Table 4. Material properties of silicon, adhesive and FR-4

Layer	Young's Modulus	Poisson's Ratio	CTE(1/ )
Silicon	112.4(Gpa)	0.28	2.62ppm
Adhesive Layer	3.45(Gpa)	0.4	10ppm
FR-4	18.2(Gpa)	0.19	16ppm

Table 5. Theory prediction ability at the free edge in trilayer structure

Material Combination: Upper Layer (Silicon) +Middle Layer (Adhesive)+Lower Layer (Fr-4)			
Theory	Pao	Jiang	Wang
Shearing Stress	Better	Not suitable	Not suitable
Peeling Stress	Not suitable	Better	Better